

# Spin-polarized tunneling as a probe of (Ga,Mn)As electronic properties

M. Elsen,<sup>1,\*</sup> H. Jaffrès,<sup>1</sup> R. Mattana,<sup>1</sup> L. Thevenard,<sup>2</sup> A. Lemaitre,<sup>2</sup> and J.-M. George<sup>1</sup>

<sup>1</sup>*Unité Mixte de Physique CNRS/Thales, Route Départementale 128,*

*91767 Palaiseau Cedex, France and Université Paris-Sud 11, 91405 Orsay, France*

<sup>2</sup>*Laboratoire de Photonique et de Nanostructures, Route de Nozay, 91460 Marcoussis, France*

(Dated: February 1, 2008)

We present magnetic and tunnel transport properties of (Ga,Mn)As/(In,Ga)As/(Ga,Mn)As structure before and after adequate annealing procedure. The conjugate increase of magnetization and tunnel magnetoresistance obtained after annealing is shown to be associated to the increase of both exchange energy  $\Delta_{exch}$  and hole concentration by reduction of the Mn interstitial atom in the top magnetic electrode. Through a 6x6 band  $k.p$  model, we established general phase diagrams of tunneling magnetoresistance (TMR) and tunneling anisotropic magnetoresistance (TAMR) *vs.* (Ga,Mn)As Fermi energy ( $E_F$ ) and spin-splitting parameter ( $B_G$ ). This allows to give a rough estimation of the exchange energy  $\Delta_{exch}=6B_G \simeq 120$  meV and hole concentration  $p \simeq 1.10^{20} \text{cm}^{-3}$  of (Ga,Mn)As and beyond gives the general trend of TMR and TAMR *vs.* the selected hole band involved in the tunneling transport.

PACS numbers: 72.25.Dc ; 75.47.-m ; 75.50.Pp

## I. INTRODUCTION

In the field of spintronics, the  $p$ -type ferromagnetic semiconductor (Ga,Mn)As offers many advantages to study tunnel magnetotransport properties when used as an electrode. The complexity of the transport mechanisms associated with spin-orbit coupled states make this material a powerful means for finding novel effects and provides new challenges for theoretical understandings. This includes tunnel magnetoresistance (TMR) across single and double barriers,<sup>1,2</sup> tunnel anisotropic magnetoresistance (TAMR),<sup>3,4</sup> Coulomb blockade anisotropic magnetoresistance<sup>5</sup> and current induced magnetization switching.<sup>6,7</sup> However one of the main limitation of this  $p$  type material for spintronic integration is the relatively low Curie temperature. Through low temperature annealing treatment after growth, Curie temperatures of 173 K can be obtained.<sup>8</sup> Elimination of interstitial manganese atoms which are double donors and which couple antiferromagnetically with the manganese atom in substitutional position, is mainly invoked. These atoms diffuse towards the surface to form either a  $\text{MnO}^{9,10}$  or a  $\text{MnN}^{11}$  layer, depending on annealing conditions.

In this paper we describe the effect of annealing on the magnetic and electric properties of a (Ga,Mn)As/(In,Ga)As/(Ga,Mn)As tunnel junction. We have focused our report on this single structure even though other junctions with different Mn concentrations and ferromagnetic layer thicknesses were studied, leading to the same general conclusion.<sup>12</sup> In the first part we detail the effect of annealing on magnetization measurements and confirm observations made on a (Ga,Mn)As trilayer structure with a GaAs barrier.<sup>13</sup> The second part presents the results obtained on junctions fabricated by optical lithography and describes the behaviour of Resistance Area (R.A) product, Tunnel Magnetoresis-

tance (TMR) and Tunnel Anisotropic Magnetoresistance (TAMR) through annealing. In the last part, a general interpretation of the data behaviour from both magnetic and electric measurements, is given through a 6x6 band  $k.p$  model of the tunneling transport. Two important parameters are identified, the Fermi energy and the spin splitting parameter  $B_G$  introduced in the framework of the Zener model in the mean-field approach.<sup>14</sup>

## II. EXPERIMENTAL RESULTS

$\text{Ga}_{0.926}\text{Mn}_{0.074}\text{As}$  (80nm)/  $\text{In}_{0.25}\text{Ga}_{0.75}\text{As}$  (6nm)/  $\text{Ga}_{0.926}\text{Mn}_{0.074}\text{As}$  (15nm) structure is grown by molecular beam epitaxy at 250 °C on a  $p$ -doped GaAs buffer layer ( $p \simeq 2 \cdot 10^{19} \text{cm}^{-3}$ ). Annealing treatment has been realized at 250 °C in a nitrogen atmosphere during 1 hour. The annealing was performed on a whole piece of 5x5 mm<sup>2</sup> for magnetic measurements whereas realised on patterned junctions for electrical experiments.

Figure 1 presents magnetization behaviour before and after annealing by SQUID (Superconducting Quantum Interference Device) measurements. The two step magnetization reversal along [100] axis at 10 K is due to the consecutive reversal of the two magnetic layers [Fig. 1a]. As a function of annealing, three important characteristics, consistent with the reduction of Mn interstitials in the top magnetic layer, can be extracted from those measurements : a large decrease of the coercivity  $H_C$  as well as an increase of the magnetic moment  $M_S$  and of the Curie temperature  $T_C$ . Concerning the variation of the  $H_C$ , magnetization study pointed out that this decrease may be due to an elimination of interstitial manganese (double donors) pinning center.<sup>15</sup> The resulting increase of the carrier concentration may also contribute to the decrease of the anisotropy field.<sup>14</sup> Considering that only the top layer is affected by annealing, through its linear

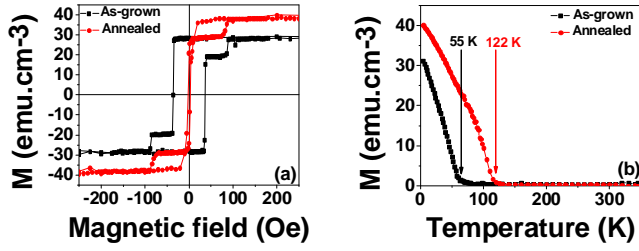


FIG. 1: (Color online) (a) Magnetization measurements *vs.* magnetic field at 10 K before and after annealing along [100] direction; (b) Magnetization measurements as a function of the temperature before and after annealing in a field of 500 Oe.

dependence on the magnetization saturation value, the spin splitting parameter increases from 17 meV (before annealing) to 24 meV (after annealing). The values of the spin splitting were estimated through the relationship  $B_G = \frac{A_F \beta M_S}{6g\mu_B}$  derived from the mean field theory, where  $A_F$  is the Fermi Liquid parameter and  $\beta$  the  $p$ - $d$  exchange integral.<sup>14</sup>

The observed Curie temperature are in good agreement with those found on thicker magnetic layers confirming that layer width larger than 50 nm should still have a high concentration of manganese interstitials.<sup>10,16</sup> In the present case, the Curie temperature goes from 55 K to 122 K [Fig. 1(b)]. Due to the higher magnetic moment of the top layer, the behaviour of the thin bottom layer is hidden, supporting the results that only the top layer properties change. A further confirmation that annealing does not act on the bottom layer comes from Auger measurements, not presented here. A strong manganese accumulation at the top of the surface is measured, whereas no obvious change in the bottom layer is observed, already put forward by Chiba *et al.*<sup>13</sup> Capping (Ga,Mn)As layer by a simple GaAs layer which width exceeds 5 nm, does not improve the Curie temperature of the simple magnetic layer<sup>17</sup> and does though support our results. The formation of a  $p$ - $n$  junction avoiding the migration of interstitial  $n$ -type manganese has been suggested.<sup>18</sup>

Magnetic tunnel junctions have been patterned by optical lithography (size of the junctions were between 8 and 128  $\mu\text{m}^2$ ). With standard dc technique the resistance of the junctions is measured at 3K and at low bias (1 mV) in the CPP (Current Perpendicular to Plane) regime. Non-linear I(V) curve indicates that a 6 nm (In,Ga)As layer still acts as a barrier.<sup>7</sup> The reason is on the one hand that the Mn acceptor level in GaAs leads to a positive band offset in (Ga,Mn)As compared to GaAs. On the other hand the well-known As antisites incorporated during the low growth process should probably govern the pinning of the Fermi level and a higher barrier than the simple Mn acceptor state may be expected. In figure 2(a) we note an increase of TMR

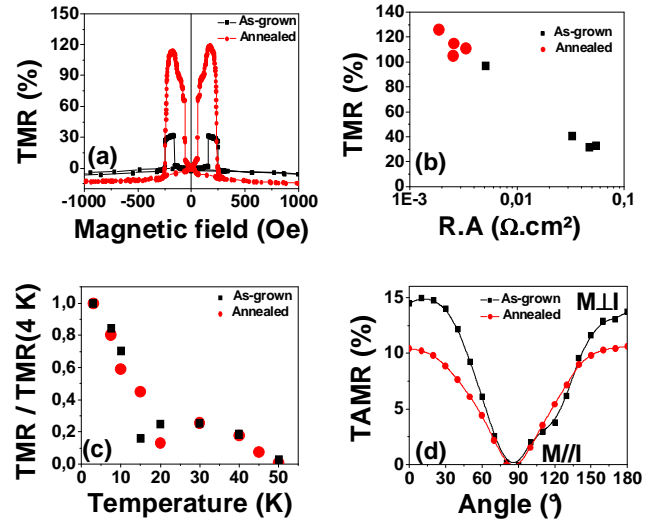


FIG. 2: (Color online) (a) Tunnel magnetoresistance measurements as a function of the magnetic field at 1 mV and 3K for a 128  $\mu\text{m}^2$  junction. (b) Tunnel magnetoresistance measurements as a function of Resistance.Area product at 3 K for 4 (un)annealed junctions. (c) Tunnel magnetoresistance at 1 mV as a function of the temperature before and after annealing. (d) Tunnel anisotropic magnetoresistance measurements as a function of the magnetic field at 1 mV and 3K.

from 30% before annealing to 120% after annealing on a 128  $\mu\text{m}^2$  junction (along [100] direction) while R.A product decreases from 0.047 to 0.003  $\Omega\cdot\text{cm}^2$ . Lowering R.A. product should be related to a change in the Fermi energy which involve a reduction of the barrier height or the barrier width and then must be associated to an increase of the hole concentration. In addition, as already observed on magnetic properties, the coercive field of the top magnetic layer changes after annealing; the difference of those values between magnetic and transport measurements is related to size effects. The same behaviour has been observed on all 4 measured junctions [Fig. 2(b)]: Whereas TMR values lay between 30% and 90% before annealing, an homogenization of the values occurs after annealing where TMR ranges between 110% and 130%. No assymetry of TMR between positive and negative applied bias has been measured after annealing.

However, we must emphasize that magnetic properties derive from the whole magnetic layers (volume effect), whereas electric properties should mainly depend on the interfaces between the tunnel barrier and the electrodes. It results that evaluating the change of the electronic properties for each magnetic layers from transport measurements appears more complex than in the case of magnetic experiments. Nevertheless, some conclusions can be drawn from TMR measurements *vs.* temperature, taking into account that the elementary process is a spin-conservative direct tunneling, i.e. the evolution of TMR with temperature is directly linked to the effective

carrier spin polarization of the ferromagnetic layer.<sup>19</sup> We note that the effective temperature at which TMR cancels remains unchanged after annealing [Fig.2(c)]. This feature comes from the magnetic properties of the bottom electrode which are not modified after annealing ( $T_C \sim 55$  K). The drop of TMR around 15 K before and after annealing is related to the quick variation of the coercive field of the thin magnetic layer as a function of the temperature.<sup>20</sup>

On the other hand, how behaves the tunnel anisotropic magnetoresistance (TAMR)? TAMR generally traduces a variation of resistance *vs.* the crystalline orientation of the electrode magnetization. In this case, this originates from the anisotropy of the valence band of (Ga,Mn)As. Careful attention was paid on the resistance difference when the magnetization is aligned along [100] (in plane magnetization) or [001] (out of plane magnetization) which leads to maximum TAMR effect in our samples. In a saturating field of 6 kOe variations are almost equal to 10-15% before and after annealing [Fig. 2(d)], in good agreement with experiments obtained on a ZnSe barrier.<sup>4</sup> When driving experiments in the plane of the layer resistance variations as small as 4% were recorded.

Combination of magnetization and transport measurements let us therefore presume that the spin splitting and the Fermi energy play an important role in tunneling transport. The influence of those parameters will be discussed now through a 6x6 band *k.p* modelisation of spin-orbit coupled states tunneling transport.

### III. THEORETICAL MODEL

Our calculations of the transmission coefficient are based on the multiband transfer matrix technique developed in details by Pethukov *et al.*<sup>21</sup>, Brey *et al.*<sup>22</sup> and Krstajic *et al.*<sup>23</sup> and applied to the hole 6x6 valence band *k.p* Hamiltonian  $H_h$ . Added to the Kohn-Luttinger kinetic Hamiltonian, this includes a *p-d* exchange term introduced by the interaction between the localized Mn magnetization and the holes derived in the mean-field approximation thus giving:

$$H_h = -(\gamma_1 + 4\gamma_2)k^2 + 6\gamma_2 \sum_{\alpha} L_{\alpha}^2 k_{\alpha}^2 + 6\gamma_3 \sum_{\alpha \neq \beta} (L_{\alpha} L_{\beta} + L_{\beta} L_{\alpha}) k_{\alpha} k_{\beta} + \lambda_{so} \vec{L} \cdot \vec{S} + 6B_G \hat{m} \cdot \vec{S} \quad (1)$$

equivalent to the one proposed by Dietl *et al.*<sup>14</sup> and Abolfarh *et al.*<sup>24</sup>. Here,  $\alpha = \{x, y, z\}$ ,  $L_{\alpha}$  are  $l = 1$  angular momentum operators,  $\vec{S}$  is the vectorial spin operator,  $\hat{m}$  the unit magnetization vector and  $\gamma_i$  are Luttinger parameters of the host semiconductor GaAs.  $6B_G$  represents the spin-splitting between the heavy holes at the  $\Gamma_8$  point like originally introduced by Dietl *et al.*<sup>14</sup> We do not take explicitly into account the stress hamiltonian which is shown to give the same qualitative conclusions.

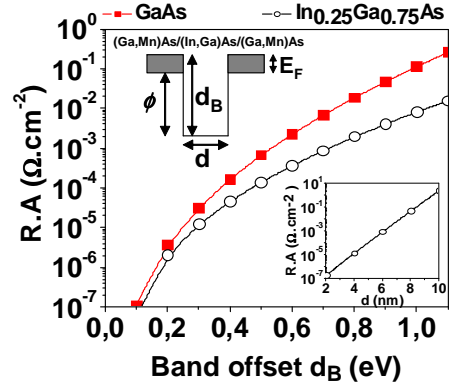


FIG. 3: (Color online) Calculated Resistance.Area (R.A) product of the trilayer structure as a function of the band offset  $d_B$  between the ferromagnetic semiconductor and a 6 nm barrier of GaAs or (In,Ga)As. Insets : (Bottom) R.A. product as a function of the (In,Ga)As barrier width  $d$ . (Top) Valence band profile of the considered heterostructure.

To derive the transmission coefficient, the boundary conditions to match at each interface are<sup>21</sup>:

i) the continuity of the 6 components of the envelope function according to  $\psi_n^+ + \sum_{\bar{n}} r_{n,\bar{n}} \psi_{\bar{n}}^- = \sum_{n'} t_{n,n'} \psi_{n'}^+$ , where the subscript  $t_{n,n'}$  ( $r_{n,\bar{n}}$ ) refer to the respective transmission (reflection) amplitude from *incident* ( $n$ ), *reflected* ( $\bar{n}$ ) and *transmitted* ( $n'$ ) waves together with

ii) the continuity of the 6 components of the current wavevector according to  $\hat{J} \psi_n^+ + \sum_{\bar{n}} r_{n,\bar{n}} \hat{J} \psi_{\bar{n}}^- = \sum_{n'} t_{n,n'} \hat{J} \psi_{n'}^+$ , where, in the *k.p* approach, the current operator in the  $z$  direction writes  $\hat{J} = \frac{1}{\hbar} \frac{\partial H_h}{\partial k_z}$ .

Concerning the heterostructure itself, the valence band offset (VBO),  $d_B$ , between (Ga,Mn)As and (In,Ga)As fixes the effective barrier height  $\phi$  according to  $d_B = -E_F + \phi$  where  $E_F \sim -0.18$  eV is the Fermi level within (Ga,Mn)As calculated from the top of the (Ga,Mn)As valence band [Inset Fig.3]. On figure 3, we present the calculated R.A product *vs.* the respective valence band offset using standard Landauer formula of conductance for 6 nm GaAs and  $\text{In}_{0.25}\text{Ga}_{0.75}\text{As}$  barriers. Although the VBO between  $\text{Ga}_{0.926}\text{Mn}_{0.074}\text{As}$  and  $\text{In}_{0.25}\text{Ga}_{0.75}\text{As}$  is still unknown, recent photoemission spectra determined the barrier height  $\phi$  between (Ga,Mn)As and GaAs to 450 meV,<sup>25</sup> in agreement with our *k.p* model considering a R.A product approaching  $\sim 10^{-3} \Omega.\text{cm}^2$  [Fig. 3] and like obtained experimentally by Chiba *et al.*<sup>20</sup> The relative small band offset between valence band of GaAs and (In,Ga)As inferior to 50 meV,<sup>26</sup> makes then such value of  $\phi \simeq 450$  meV a plausible order of magnitude for the effective barrier height for  $\text{In}_{0.25}\text{Ga}_{0.75}\text{As}$  matching with the R.A product after annealing. However, in the present case, the real value of  $\phi$  may vary depending on:

i) the nature and density of the dangling bonds at the interfaces promoted by the low-temperature growth procedure.<sup>27</sup>

ii) the local density and position in energy of ionized defects such as As antisites in the barrier which strongly influences the valence band bending of the whole heterostructure.

However, surprisingly, we have noticed that TMR remains quasi insensitive to the barrier height  $\phi$  (not shown). Let us then focus on the phase diagrams TMR ( $E_F$ ,  $B_G$ ) and TAMR ( $E_F$ ,  $B_G$ ) established from the preceding model of  $k.p$  tunnel conduction. Figure 4 displays both TMR and TAMR *vs.* the spin splitting parameter  $B_G$  and the Fermi energy  $E_F$  of the ferromagnetic semiconductor whose properties are assumed to be identical at both sides of the (In,Ga)As barrier. The zero energy for  $E_F$  corresponds here to the top of the valence band for (Ga,Mn)As in its paramagnetic phase ( $B_G=0$ ). Also are plotted on phase diagrams 3 different lines corresponding to constant carrier concentrations of  $1 \cdot 10^{20} \text{ cm}^{-3}$ ,  $3.5 \cdot 10^{20} \text{ cm}^{-3}$  and  $5 \cdot 10^{20} \text{ cm}^{-3}$ , as well as the energy of the four first bands at the center of the Brillouin zone. Let us first emphasize on the general trends for TMR and TAMR from such diagrams.

#### IV. DISCUSSION

High TMR values, up to several hundred percents, can be expected either for spin splitting values larger than several tens of meV or for low carrier concentration, that is when only the first subband is involved in the tunnelling transport. This corresponds to a quasi half metallic character for (Ga,Mn)As. Starting from the first subband and increasing the carrier concentration to fill the consecutive lower subbands ( $n=2,3,4$ ), up and down spin populations start to mix up, leading to a decrease of TMR. For high carrier concentration ( $n=4$ ), small TMR is expected which may anticipate difficulties to conciliate high Curie temperature and large TMR effects. We specify that for low values of spin splitting and Fermi energy, ferromagnetic phase induced by carrier delocalization may not exist (top right corner of the diagram) which is not taken into account in our  $k.p$  modelisation (propagative envelope wave function). In the same manner, we cannot reproduce metal-insulator transition in the tunneling transport, responsible for the large TAMR obtained in in-plane geometry.<sup>3,28</sup>

What about TAMR signal? We can firstly note a possible change of sign for TAMR on crossing the third subband. The first subband clearly gives a negative contribution to TAMR. This originates from the predominant heavy hole character of such band, an in-plane magnetization allowing, through off diagonal components, a possible heavy to light hole conversion, and then a larger transmission through the barrier.<sup>29</sup> This argument is reversed for the second and third subbands with the results that TAMR becomes positive when  $n=2$  and  $n=3$  subbands are dominant in the tunneling transport. We can point out that a change of TAMR

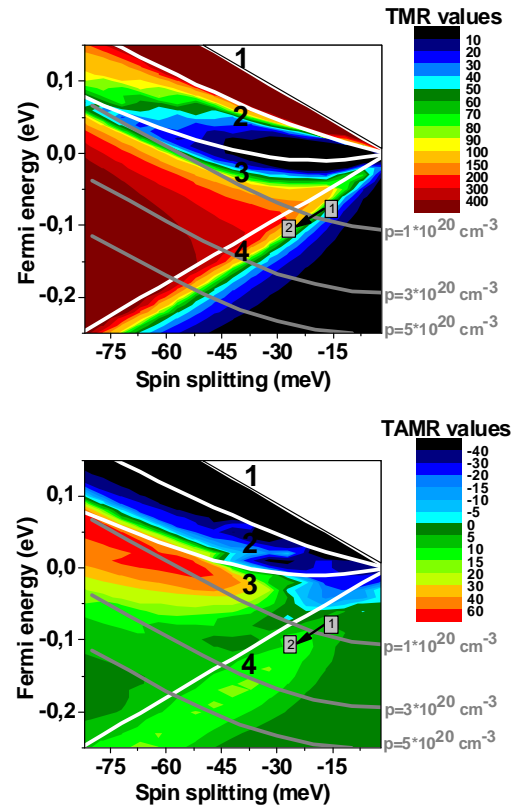


FIG. 4: (Color online) Tunnel magnetoresistance values (a) and tunnel anisotropic magnetoresistance values (b) represented as a function of the Fermi and spin splitting energy for a 6 nm (In,Ga)As barrier with a band offset of 450 meV. White lines represent the 4 bands at the center of the Brillouin zone. Gray lines indicate the Fermi energy for different hole concentrations.

sign was already observed on a Zener-Esaki diode<sup>30</sup> as well as theoretically established through tight-binding treatment.<sup>31</sup> Reducing the hole concentration through hydrogenation technique should give the possibility to probe this possible crossover from positive to negative TAMR.<sup>32</sup>

Concerning our own experiments, taking into account conjugate TMR and TAMR values obtained before and after annealing, one can roughly evaluate the projection of the corresponding signals trajectories in the  $[E_F, B_G]$  plane followed during annealing [Fig.4]. A good qualitative agreement can be found even though symmetrical junctions were simulated in order to restrict the number of parameters.

Evaluating directly the interfacial spin splitting from the mean field theory appears difficult since the interfacial magnetic properties are hardly accessible. However, when using the estimated  $B_G$  value of the top magnetic electrode (before and after annealing) a good qualitative agreement can be found for TMR

and TAMR, as illustrated by the trajectory in figure 4 between point 1 (before annealing) and point 2 (after annealing). A more refine calculation including two different  $B_G$  after annealing should be required to draw definite quantitative conclusion.

We are now going to discuss the hole concentration derived from these diagrams. TMR and TAMR values obtained before annealing are well reproduced for a hole concentration approaching  $10^{20}\text{cm}^{-3}$ , in good agreement with the one measured for single (Ga,Mn)As layer and already reported.<sup>33</sup> The annealing procedure has for effect to *i*) remove Mn interstitial atoms, *ii*) increasing carrier concentration and *iii*) reduce the effective barrier height even if the valence band position is expected to rise due to an increase of the average exchange energy ( $B_G$ ). The large reduction of the R.A product together with the increase of TMR are consistent with such assumption. Nevertheless, the hole concentration extracted after annealing from the phase diagram  $\sim 1,7 \cdot 10^{20}\text{cm}^{-3}$  appear to be weak compared to the one reported in the literature and derived from Hall effect measurements. The existence of a possible concentration gradient can be at the origin of such discrepancy. Also can be invoked, a reduction of the hole concentration at the interfaces with the barrier due to a significant charge transfer between *p*-type (Ga,Mn)As and *n*-type (In,Ga)As (excess of As antisites).<sup>28,34</sup>

## V. CONCLUSION

In summary we have shown that annealing a (Ga,Mn)As-based tunnel junction mainly affects the

properties of the top magnetic layer, ensuring an increase of the effective magnetization and a significant enhancement of the tunnel magnetoresistance. The confrontation between experiments and modelisation performed within a 6x6 band k.p treatment *vs.* intrinsic (Ga,Mn)As parameters (hole filling, exchange energy) allowed a rough estimation of the average exchange interactions and carrier concentration in (Ga,Mn)As at the interface with the barrier. We point out that while the magnitude of TMR appears very sensitive to both parameters ( $B_G$  and  $E_F$ ), the TAMR variation is limited to several tens of percent but may change sign crossing from upper to lower (Ga,Mn)As subbands. As a final conclusion, we think that this reduced parameter model gives a good qualitative agreement of the tunneling transport and enables to extract the fundamentals of TMR and TAMR processes involving tunnel transport of spin-orbit couple state. In order to go further and draw more quantitative information, a perfect control and knowledge of the carrier density seems to be necessary.

## Acknowledgments

We gratefully acknowledge H.-J. Drouhin, A. Fert, G. Fishman and B. Vinter for fruitful discussions.

This work was supported by the EU Project NANOSPIN FP6-2002-IST-015728 and by the french ANR Program of Nanosciences and Nanotechnology (PNANO) project MOMES.

---

\* Electronic address: marc.elsen@paris7.jussieu.fr

<sup>1</sup> M. Tanaka and Y. Higo, Phys. Rev. Lett. **87**, 026602 (2001).

<sup>2</sup> R. Mattana, J.-M. George, H. Jaffrès, F. N. V. Dau, A. Fert, B. Lépine, A. Guivarc'h, and G. Jezequel, Phys. Rev. Lett. **90**, 166601 (2003).

<sup>3</sup> C. Ruster, C. Gould, T. Jungwirth, J. Sinova, G. M. Schott, R. Giraud, K. Brunner, G. Schmidt, and L. W. Molenkamp, Phys. Rev. Lett. **94**, 027203 (2005).

<sup>4</sup> H. Saito, S. Yuasa, and K. Ando, Phys. Rev. Lett. **95**, 086604 (2005).

<sup>5</sup> J. Wunderlich, T. Jungwirth, B. Kaestner, A. C. Irvine, A. B. Shick, N. Stone, K.-Y. Wang, U. Rana, A. D. Giddings, C. T. Foxon, et al., Phys. Rev. Lett. **97**, 077201 (2006).

<sup>6</sup> D. Chiba, Y. Sato, T. Kita, F. Matsukura, and H. Ohno, Phys. Rev. Lett. **93**, 216602 (2004).

<sup>7</sup> M. Elsen, O. Boulle, J.-M. George, H. Jaffrès, R. Mattana, V. Cros, A. Fert, A. Lemaitre, R. Giraud, and G. Faini, Phys. Rev. B **73**, 035303 (2006).

<sup>8</sup> K. Y. Wang, R. P. Campion, K. W. Edmonds, M. Sawicki,

T. Dietl, C. T. Foxon, and B. Gallagher, Proc. 27th Int. Conf. on Phys. of Semicon., Flagstaff, AZ, USA p. 333 (July 2004, (New York 2005)).

<sup>9</sup> K. W. Edmonds, P. Boguslawski, K. Y. Wang, R. P. Campion, S. N. Novikov, N. R. S. Farley, B. L. Gallagher, C. T. Foxon, M. Sawicki, T. Dietl, et al., Phys. Rev. Lett. **92**, 037201 (2004).

<sup>10</sup> K. M. Yu, W. Walukiewicz, T. Wojtowicz, I. Kurykiszyn, X. Liu, Y. Sasaki, and J. K. Furdyna, Phys. Rev. B **65**, 201303 (2002).

<sup>11</sup> B. J. Kirby, J. A. Borchers, J. J. Rhyne, S. G. E. te Velthuis, A. Hoffmann, K. V. O'Donovan, T. Wojtowicz, X. Liu, W. L. Lim, and J. K. Furdyna, Phys. Rev. B **69**, 081307(R) (2004).

<sup>12</sup> M. Elsen, PhD thesis, Universit Pierre et Marie Curie (Paris VI) (2007).

<sup>13</sup> D. Chiba, K. Takamura, F. Matsukura, and H. Ohno, Appl. Phys. Lett. **82**, 3020 (2003).

<sup>14</sup> T. Dietl, H. Ohno, and F. Matsukura, Phys. Rev. B **63**, 195205 (2001).

<sup>15</sup> S. J. Potashnik, K. C. Ku, R. F. Wang, M. B. Stone,

- N. Samarth, P. Schiffer, and S. H. Chun, *J. Appl. Phys.* **93**, 6784 (2003).
- <sup>16</sup> K. M. Yu, W. Walukiewicz, T. Wojtowicz, W. L. Lim, X. Liu, U. Bindley, M. Dobrowolska, and J. K. Furdyna, *Phys. Rev. B* **68**, 041308 (2003).
  - <sup>17</sup> M. B. Stone, K. C. Ku, S. J. Potashnik, B. L. Sheu, N. Samarth, and P. Schiffer, *Appl. Phys. Lett.* **83**, 4568 (2003).
  - <sup>18</sup> B. J. Kirby, J. A. Borchers, J. J. Rhyne, K. V. O'Donovan, T. Wojtowicz, X. Liu, Z. Ge, S. Shen, and J. K. Furdyna, *Appl. Phys. Lett.* **86**, 072506 (2005).
  - <sup>19</sup> R. Mattana, M. Elsen, J.-M. George, H. Jaffrès, F. N. V. Dau, A. Fert, M. F. Wyczisk, J. Olivier, P. Galtier, B. Lépine, et al., *Phys. Rev. B* **71**, 075206 (2005).
  - <sup>20</sup> D. Chiba, F. Matsukura, and H. Ohno, *Physica E* **21**, 966 (2004).
  - <sup>21</sup> A. G. Pethukov, A. N. Chantis, and D. O. Demchenko, *Phys. Rev. Lett.* **89**, 107205 (2002).
  - <sup>22</sup> L. Brey, C. Tejedor, and J. Fernandez-Rossier, *Appl. Phys. Lett.* **85**, 1996 (2004).
  - <sup>23</sup> P. Krstajic and F. M. Peeters, *Phys. Rev. B* **72**, 125350 (2005).
  - <sup>24</sup> M. Abolfath, T. Jungwirth, J. Brum, and A. H. MacDonald, *Phys. Rev. B* **63**, 054418 (2001).
  - <sup>25</sup> M. Adell, J. Adell, L. Ilver, J. Kanski, and J. Sadowski, *Appl. Phys. Lett.* **89**, 172509 (2006).
  - <sup>26</sup> S. Tiwari and D. J. Frank, *Appl. Phys. Lett.* **60**, 630 (1992), if one takes into account explicitly the stress between (Ga,Mn)As and (In,Ga)As, this shift should correspond to the valence band offset between (Ga,Mn)As and the LH component of (In,Ga)As that is preferentially transmitted through thick barriers.
  - <sup>27</sup> S. Lodhaa, D. B. Janes, and N.-P. Chen, *J. Appl. Phys.* **93**, 2772 (2003).
  - <sup>28</sup> K. Pappert, M. J. Schmidt, S. Humpfner, C. Ruster, G. Schott, K. Brunner, C. Gould, G. Schmidt, and L. Molenkamp, *Phys. Rev. Lett.* **97**, 186402 (2006).
  - <sup>29</sup> M. Elsen (unpublished).
  - <sup>30</sup> R. Giraud, M. Gryglas, L. Thevenard, A. Lemaitre, and G. Faini, *Appl. Phys. Lett.* **87**, 242505 (2005).
  - <sup>31</sup> P. Sankowski, P. Kacman, J. Majewski, and T. Dietl, *Phys. Rev. B* **75**, 045306 (2007).
  - <sup>32</sup> L. Thevenard, L. Largeau, O. Mauguin, A. Lemaitre, and B. Theys, *Appl. Phys. Lett.* **87**, 182506 (2005).
  - <sup>33</sup> M. Malfait, J. Vanacken, W. V. Roy, G. Borghs, and V. Moshchalkov, *J. Magn. Magn. Mater.* **290**, 1387 (2005).
  - <sup>34</sup> A. Koeder, S. Frank, W. Schoch, V. Avurtin, W. Limmer, K. Thonke, R. Sauer, M. Krieger, K. Zuern, P. Ziemann, et al., *Appl. Phys. Lett.* **82**, 3278 (2003).